Evolution of particle breakages for calcareous sands during ring shear tests

Houzhen Wei[1], Tao Zhao[2, 3*], Jianqiao He[4], Qingshan Meng[1], Xinzhi Wang[1]

[1] State Key Laboratory Geomechanics and Geotechnical Engineering, Institute of Rock and Soil Mechanics, Chinese Academy of Sciences, Wuhan, 430071, China

[2] Key Laboratory of Geotechnical and Underground Engineering (Tongji University), Ministry of Education, Shanghai, 200092, China

[3] State Key Laboratory of Hydraulics and Mountain River Engineering, College of Water Resource and Hydropower, Sichuan University, Chengdu, 610065, China

[4] Guangxi Road and Bridge Engineering Group Co., Ltd, Nanning, 530011, China

* Corresponding author: Tel.: +86 28 8540 6701 E-mail: zhaotao@scu.edu.cn

Abstract: Ring shear tests were performed in this work to investigate the characteristics of shear band formation and particle breakages for calcareous sands sampled from the South China Sea. The tests focused on the formation of shear band and the evolution of particle breakages under various loading stress levels, together with the sensitivity analyses on the initial sample grading and shear rate. The breakage of particles has a significant influence on the stress-strain relationship, volumetric deformation and the final grading of calcareous sands. In particular, the calcareous sand specimen tends to remain a constant volume and a stable grading at shear strains larger than 2000%. The change of the micro-structure of calcareous sands during shearing has been illustrated by the Scanning Electron Microscopy (SEM) images, showing clear evolution of particle breakage and surface smoothness within the shear band. A considerable amount of fine particles (<0.074 mm) were produced during the tests, and the final complete particle size distribution can be obtained by the laser diffraction particle size analyzer. The findings of this study improve the understanding of calcareous sands that they can be crushed readily under normal loading stress level as long as the shear strain continues.

Keywords: ring shear test, calcareous sands, shear band, particle breakage, SEM

Introduction

Calcareous sands are deposits widely found in tropical marine environment. They have significantly different physical and mechanical properties from their terrigenous counterpart soils, such as particle angularity, high crushability, large internal voids, and weakly cemented soil structure (Wang et al., 2017). These unique properties are preferred for particle breakage which has been recognized as the most important feature of calcareous sands, controlling soil strength, deformation and permeability (David et al., 2011, Shahnazari and Rezvani, 2013). In fact, the breakage of calcareous sands has been widely observed in offshore engineering practices under certain stress and strain conditions, for either weak (e.g. calcareous or carbonate sands) or strong (e.g. quartz sand) soil particles (Coop et al., 2004, Donohue et al., 2009, Miao and Airey, 2013, Qadimi and Coop, 2007, Wu et al., 2014, Yu, 2017). Among others, the changes of particle shape, surface roughness and particle size distribution (PSD) are the most notable characteristics of particle breakage. As noted by Cho et al. (2006) and Altuhafi and Coop (2011), after breakage, the irregular particles tend to evolve towards a spherical shape and median surface roughness, with lower aspect ratios than the original particles.

During compression or shearing, particle breakages usually occur once the loading stress exceeds the yielding stress of sands (Hyodo et al., 2002, Lade et al., 1996, McDowell, 2002, Sebastian et al., 2006). This effect is particularly evident for uniformly graded samples (Bolton et al., 2008). For non-uniformly graded grains, McDowell and Bolton (1998) observed that fine grains can be crushed successively under increasing loading stresses, while the coarse grains can resist fractures due to their high coordination numbers. Einav (2007) also stated that the large particles are more resistive to crushing during the compression of a dense packing of poly-dispersed granular materials because they can get cushioned by the surrounding fine grains. However, this observation contradicts the generally accepted trend of particle strength increasing with decreasing size (Hardin, 1985), because in the case of dense granular packing, the forces transferring at contacts (i.e. the efficiency is reflected by coordination number) are dominant and the potential defects (e.g. fractures or joints) within the solids are not considered. Altuhafi and Coop (2011) examined the influence of particle density and initial grading on the mechanical responses of crushable sands by one-dimensional compression tests. They observed that a significant amount of particle breakages occurred in poorly graded samples, while little breakage can be found in very well-graded samples.

Hardin (1985) proposed that the potential for breakage increases with the particle size, and can be quantified effectively by using relative breakage. This parameter has been proved to be independent of particle size distribution, while it depends primarily on particle shape, granular packing state, effective stress and presence of water. To get a fully unified correlation with various tests, Lade et al. (1996) proposed the particle breakage factor, B_{10}, based on the D_{10} particle size, to correlate with the total energy input. Thus, the amount of crushed particles can be predicted if the stress and strain relationship of a soil specimen can be readily obtained. Zhang et al. (2015) used a simple two-parameter model to describe particle size distribution generated from breakages of initial uniformly graded sand samples. In this model, various particle breakage patterns can be captured by the modified two-parameter Weibull distribution function, including asperity breakage and particle splitting. In addition, the breakage pattern of initially non-uniformly graded particles can be considered as a collection of uniformly graded particles with the crushing state of each particle size group following the Weibull distribution.

In experimental investigations, the ring shear (RS) tests are superior to triaxial compression and direct shear tests for the extremely large shear strains reached. Luzzani and Coop (2002) observed that large shear deformation occurs before a stable grading can be achieved in ring shear tests. They also suggested that the constant volume state observed in triaxial compression tests should result from the counteracting components of volumetric strain, instead of the completion of particle breakage. Sadrekarimi and Olson (2010) studied the formation of shear band during ring shear tests, and concluded that the localization of non-uniform deformation occurs just before the mobilization of peak shear resistance. After failure, the shear displacements localized only within the shear band of a width of 10 to 14 times the median particle size (D_{50}). Fukuoka et al. (2007) conducted drained RS tests on sands, and found that high shear speed would lead to reduced friction angle, and particle breakage intensity increases with the normal consolidation stress level.

Though lots of efforts have been devoted to investigate the shear band formation and the corresponding particle breakage under various testing conditions, detailed analyses of shear band evolution and soil micro-structure changes are still lacking. These limitations prompt the more systematic research on calcareous sands, with the purpose to highlight particle breakage characteristics under various conditions, as presented herein. The paper is organized as follows: firstly, the experimental configurations are given. Then, the analyses of experimental data are presented, with respect to the stress-strain relationship, sample deformation and sand breakage characteristics. The final section summarizes major conclusions reached in this study.

Experimental configurations

The current study employed the ring shear tests to investigate the mechanical and deformation behaviour of calcareous sands under relatively large shear displacement and high shear speed. The sand specimens were sampled from Yongshu Coral Reef, South China Sea (Wang et al., 2011). The ring shear (RS) testing apparatus used in this study is shown in Figure 1. The calcareous sand specimen is placed in the shear box, with dimensions of 150 mm of outer diameter (OD), 100 mm of inner diameter (ID), and 20 mm of height. The sectional area is 98.17 cm^2. The testing apparatus allows the application of the shear torque of up to 400 N·m, and the vertical loading stress of up to 500 kPa. The rotational speed ranges from 0.0005°/min to 50°/min, which corresponds to a horizontal displacement rate of 0.00054 mm/min to 54.5 mm/min.

For all tests performed in this study, the consolidated and drained (CD) conditions were employed to consider the process of pile driving in calcareous sands at relatively high shear speeds (see also Table 1). In addition, as noted by Coop et al. (2004) and others, during shearing, the uniformly graded sands have much higher breakage intensities than the well-graded sands. Thus, the uniformly graded sand specimens of sieve interval 0.5-1 mm were used in most of tests to maximize particle breakage. In the current analyses, the shear strain is calculated as: $\gamma=\delta h/C$, with δh being the horizontal shear displacement, C being the mean circumference of the specimen. According to Coop et al. (2004), the volumetric strain (ε_v) can be calculated via the axial (vertical) deformation, because the radial deformation is nil as confined by the shear box. It is thus defined as $\varepsilon_v=\delta v/H_0$, with δv being the vertical displacement, H_0 being the initial sample height. For a comprehensive study on the shearing behavior of calcareous sands, the following experimental configurations were employed:

1) Vertical loading stress and shear strain: calcareous sand specimens with size grading of [0.5, 1] mm were tested under the vertical loading stresses of 200 kPa, 300 kPa and 400 kPa, respectively. Different final shear strains were set for these tests (see Table 1). The shear rate is constant as 43.6 mm/min for all tests.

2) Material property: three sets of calcareous sand samples were tested, including two uniformly graded samples of [0.5, 1] and [1, 2] mm, and one well-graded sample of [0.075, 2] mm, with D_{50} of 0.5 mm. In a series of tests, the vertical consolidation stresses are set as 50 kPa, 100 kPa, 200 kPa, 300 kPa, 400 kPa and 600 kPa, respectively. The final shear strain for all tests is 2546.5% (i.e. 10 m of the equivalent shear distance). The shear rate is constant as 43.6 mm/min for all tests.

3) Shear rate: the uniformly graded calcareous sand specimens of [0.5, 1] mm were tested under vertical loads of 300 kPa. The shear rate is set as 43.6 mm/min, 11 mm/min and 3.3 mm/min for three tests, respectively. The final shear strain for all tests is 509.3% (i.e. 2 m of the equivalent shear distance).

The specimen preparation and ring shear tests are in an orderly step-by-step setting-up procedure, as follows.

1) The [0.5, 1] mm uniformly graded calcareous sands are obtained via two-sieve screening. Then, the sands are washed by distill water and then dried in a drying oven. Specimens with other specific grading can be obtained in a similar way.

2) The sands are carefully poured into the bottom annular platen until the final dimensions of 150 mm OD, 100 mm ID, and 20 mm height are reached. In this process, a smooth glass rod (6 mm in diameter) will be used to stir the sands near the upper surface gently so that the aimed height can be reached

3) Distilled water is slowly poured onto the upper surface of the sand specimen, until a fully saturated state is reached. After 4 hours of self-weight consolidation, the loading and shearing systems are installed in place. Then, a light vertical seating load of 10 kPa is applied on the upper annular platen to make it contact fully with the specimen.

4) The aimed consolidation loading stress is applied on the upper platen until the sample is fully consolidated. Then, the specimen is subject to ring shear under constant rotational speed (see the defined shear rate in Table 1).

5) After the test is concluded, all loads are gradually reduced back to zero, and the loading and shearing systems are removed. The calcareous sands locating in the shear band is carefully examined via digital imaging and particle size screening, regarding the shear deformation and particle size distriubiton characteristics.

Analyses of the experimental results

The ring shear tests conducted in this research aims to clarify the formation of shear band and the evolution of particle breakage under various loading stress levels and material properties. The following analyses firstly present the results of tests with various vertical loading stresses and final shear strains. Then, the influence of initial sand grading and shear rate on the overall response of calcareous sands are analysed.

Tests with various vertical loading stress

As stated by Sadrekarimi and Olson (2010), the formation of shear band is an important factor for understanding soil failure. This unique feature together with its evolution was visualized by employing a transparent outer confining ring in their ring shear tests. However, under the current experimental configurations, a series of tests with increasing final shear strain were employed to study the formation and evolution of shear bands within the sand specimens. By this approach, it is also possible to analyse particle breakages at different loading stages in a quantitative way. A direct comparison of particle characteristics between the initial intact sands and crushed grains after the tests is shown in Figure 2. It is clear that the mean grain size of calcareous sands decreases gradually with the shear strain (e.g. for tests RS-3, RS-4 and RS-5), indicating that significant particle breakages do exist and increases with the shear strain at different stages of the tests.

Figure 3 illustrates the stress-strain relationship of the RS tests under various vertical loading stresses. According to the figure, the peak shear strength occurs at a relatively small strain of around 3.6%, and increases with the vertical loading stress. Then, the shear stress decreases quickly and it can reach the residual strength at $\gamma > 25\%$. However, apparent oscillations of stress can be clearly observed for these tests, indicating that intensive particle breakages and rearrangements may occur within the shear band. Figure 4 illustrates the evolution of volumetric strains measured for test RS-5 under different vertical loading stresses. At the beginning of the tests, the axial strain increases slightly due to the compression of the specimen. Then, the specimen would dilate sharply for a small shear displacement. This effect of volume dilation becomes very evident for tests with low stress levels. However, for tests under high stress level, the volume compression dominates the specimen deformation. For these tests, very large volumetric strains can be observed at high shear strains. This characteristics of volumetric deformation has also been observed by Coop et al. (2004), and can be ascribed to particle breakages within the shear band. The shear strain reached at the peak volumetric dilation also corresponds to the peak shear strength (see Figure 3). Further increase of shear strain would lead to specimen compression, as represented by the gradual increase of volumetric strains. As expected, the compression induced volumetric strain increases with the vertical loading stress. However, at very large shear strain ($\gamma > 1000\%$), the increase of ε_v tends to slow down for test under 400 kPa loading stress, showing a gradual stabilized volumetric deformation. This result of volumetric change has been reflected by the slight increase of residual shear strength in Figure 3. In addition, the corresponding value of γ for the stabilized volume is inversely related to the vertical loading stress. This trend agrees well with the observation by Coop et al. (2004) that tests at higher stress level can always reach the stable volumetric strain at relatively lower shear strains.

After the RS tests, the deformed specimens were taken out of the ring shear box, and images from the lateral view of the sliced specimen were taken, as shown in Figure 5. Apparent fine sand slurry can be observed in the middle of the specimen, which consists of fragmented fine calcareous sands and water. In this region, the specimen undergoes intensive shearing, and thus denoted as shear band (see the region enclosed by red dashed curves, with its height being approximately 1/3 of the deformed sample height). As stated by Coop et al. (2004), the shear band is always located in the central layer of the deformed sand sample, with a much higher breakage than the top and bottom layers. According to Figure 5, it can be observed that the shear-induced particle breakage becomes gradually evident with increasing shear strains, as shown by the smooth surface at higher shear strain. The detailed information of particle characteristics and arrangements in the shear band can be obtained by imaging via the Scanning Electron Microscopy (SEM). Here, we present images for tests under 400 kPa vertical loading stress, and with different shear strains, as shown in Figure 6. As a comparison, the image of a single coarse calcareous sand particle is also presented in Figure 6(a). According to the figure, it can be seen that the intact calcareous sand has an angular shape, with very rough surface and well-developed small voids. The porous structure is also crucial for the calcareous sands to be crushed readily into very fine grains under external loadings. At relatively small shear strains (e.g. RS-1, RS-2), the surface of the specimen is very rough with large particles and void spaces existing within the shear band. However, the surface of the shear band gradually becomes smoother at higher shear strains. This phenomenon is as expected because the increase of shear strain can lead to a much complete particle breakage in the shear band, producing a large amount of fines (< 0.074 mm). The fine sands can effectively fill up the void spaces creating very smooth surfaces.

As stated by Zhang et al. (2015), the particle size distribution (PSD) is a unique characteristics of a soil specimen, determining its physical and mechanical properties (e.g. particle size and shape, stress-strain behavior). In soil constitutive modeling, the inclusion of PSD as a variable is necessary to consider particle breakages and variations of mechanical behavior (Einav, 2007, Muir Wood and Maeda, 2007). In this study, the calcareous sands in the shear band were carefully retrieved from the shear box following each test, and then the PSDs of coarse grains were analyzed via wet-sieving by hand, while fine particles smaller than 0.074 mm were analyzed by the laser diffraction particle size analyzer. The obtained PSDs are shown in Figure 7. According to the figure, the particle breakage effect can be reflected clearly by the production of a considerable amount of particles finer than the initial minimum size of 0.5 mm. After the test, the particle size ranges from 10^{-3} mm to 1 mm, with more than 30% of newly produced fine particles. The amount of fine particles increases with the vertical loading stress, indicating that the particle breakage has a clear dependency on the stress level. As the final shear strain increases from 127.3% to 4074.4% (i.e. for the tests RS-1 to RS-6), the PSD curve shifts gradually upwards, showing continuous production of fine grains within the shear band. For tests under various loading stress levels, the resultant finest particles appear to have unique sizes, and decrease with the final shear strain. This feature shows that a unique dependency relationship between the finest crushed particle size and the final shear strain may exist. However, this relationship can also be influenced by initial particle grading and shear strain rate significantly, as will be discussed in the following analyses.

The influence of initial grading

In this study, calcareous sands with various initial grading were used in the RS tests. In particular, we used two uniformly graded samples with the absolute particle size of [0.5, 1] mm and [1, 2] mm (i.e. for tests RS-5 and RS-7 in Table 1), and one well-graded sample of [0.075, 2] mm with D_{50} of 0.5 mm (see RS-8 in Table 1 and the initial PSD curve in Figure 10). For all tests, the final shear strain was set as 2546.47% (i.e. 10 m of shear distance), and the moderate vertical loading stress of 300 kPa was used.

Figure 8 shows the evolution of shear stress with the shear strain for tests with different grading. It can be seen that the peak shear stress occurs at a relatively low shear strain (≈ 3%), and it is dominantly large for specimens consisting of uniformly graded and fine sands (e.g. RS-5). However, a completely opposite trend exists for the residual shear strength. At large shear strains, the residual shear stress oscillates intensively due to continuous particle breakages and granular structure rearrangements. This is especially true for tests RS-7 and RS-8, in which a large portion of coarse sands were presented. The magnitude of stress oscillation tunes gradually at large shear strains due to a complete breakages of coarse particles within the shear band.

Figure 9 shows the evolution of volumetric strain with the shear strain during the RS tests under a vertical loading stress of 300 kPa. It is clear that the specimen of fine and uniformly graded sands shows clear volume dilation at the beginning of the tests, while it is not evident for coarser and well-graded specimens, indicating that the coarse grained specimens can be compressed easily due to the existence of large internal void spaces. At larger shear strains, the three different specimens are all compressed, and the volumetric strain tends to converge to stable values at shear strains larger than 2000%. This phenomenon indicates that the calcareous sands in the shear band have been crushed thoroughly. This feature is particularly evident for the test RS-8 in which the final stable volumetric strain is relatively small (-27%). In this case, the total amount of coarse grains is small, and particle breakage can be completed quickly at a relatively small shear strain. The convergence of volumetric strain towards a constant value at higher shear strain has also been observed in Coop et al. (2004) in which a critical shear strain was associated with this change.

The PSDs of tests with various initial grading are illustrated in Figure 10. According to the figure, it can be observed that the PSD curves for all tests shifted towards the fine grain size range, indicating that a large portion of fine grains (< 0.074 mm) have been produced due to particle breakage. Tests RS-5 and RS-8 have very similar final grading curves, even though RS-8 has a much wider initial grading. For test RS-7, it has a much higher percentage of fine grains than the other two tests, and apparent grading discontinuity (poorly graded) can be observed for the size range of [0.1, 0.3] mm. In this case, the coarse grains have relatively lower shear strength than the finer ones, and thus the particle asperities of coarse grains can be easily crushed when sheared off by the surrounding particles. The finest particle produced by the shear-induced crushing in RS-8 is smaller than those in RS-5 and RS-7, due to much finer sand compositions in the initial specimen.

The influence of shear rate

In this study, we also tested the influence of shear rate on the response of calcareous sands. The testing conditions are listed in Table 1, as tests RS-3, RS-9 and RS-10. This kind of investigation is of practical importance as the penetration of piles into sands is normally a dynamic process, in which a wide range of shear rates can be encountered in different engineering projects. Figure 11 shows that test RS-3 with a rapid shear rate can lead to relatively high peak shear strength, while RS-9 and RS-10 have almost the same peak shear strength. In addition, RS-3 manifests much higher stress oscillations than RS-9 and RS-10 at large shear strains, showing that fast shearing would cause high perturbations to the calcareous sands. For all tests, the residual shear strengths of calcareous sands are almost the same, indicating that the residual shear strength is independent of the shear rate and might depend only on the material properties (e.g. grains size / grading, shape, surface roughness, breakage).

Figure 12 illustrates the grading curves of calcareous sands in the shear band obtained after the tests. It can be observed that a much more uniform grading curve can be obtained for slowly sheared calcareous specimen (i.e. RS-10), while fast shearing may result in poor sand grading, e.g. discontinuous grain size of [0.1-0.4] mm in RS-3. This phenomenon is as expected because during the fast shearing process, the force chains of a granular packing cannot persist for a long time as particles located in the shear band are agitated frequently due to rapid dynamic motions.

Discussion

The ring shear tests presented in this study were aimed at investigating the evolution of particle breakages by shearing calcareous sands with relatively long distances. It is apparent that the extent of particle breakage can vary significantly for different testing conditions, such as shearing distance, vertical loading stress, initial sand grading and shear rate. Thus, it is necessary to employ a unique parameter to quantify the particle breakage intensity and relate it to specific employed testing conditions. Actually, several different parameters have been proposed in the literature to study the particle breakages. Some of them focus on the increase of surface area and fragmentation energy (Locat et al., 2006, McDowell et al., 2002), while others on characterizing the change of particle size and grading via experimental and numerical approaches (Einav, 2007, Hardin, 1985, Lade et al., 1996, Richard et al., 2001). In this study, the widely accepted relative breakage (B_r) by Hardin (1985) has been adopted in the analyses due to its advantage of representing particle grading changes as a single simple parameter. The definition of B_r has been illustrated in Figure 7 (d), as the ratio of total particle breakage (area B) to the potential breakage (sum of area A and B). In this definition, the commination limit is considered as the upper limit of the silt size of 0.074 mm. In the current analyses, we also noticed that a large amount of calcareous sand particles with smaller sizes can also be crushed during the ring shear tests under normal vertical loading stress levels. Thus, the choice of this size limit can be further decreased to consider the breakage potential of even finer particles. However, as stated by Bowman et al. (2012), the choice of this size limit is rather arbitrary, and the use of a different value will simply shift the value of B_r, while the relative particle breakage intensity would keep unaltered. Thus, for consistency, the current study will just employ the same definition of relative breakage as Hardin (1985).

According to the PSD curves of each test (see Figure 7, Figure 10 and Figure 12), the relative particle breakage can be summarized as a function of the final shear strain (γ), the vertical loading stress (σ), the initial sand grading (C_u), the maximum particle size (D) and the shear rate ($\dot{\gamma}$), as shown in Eq. (1).

$$B_r = f\left(\gamma,\ \sigma,\ C_u,\ D,\ \dot{\gamma}\right) \tag{1}$$

where C_u is the coefficient of uniformity ($=d_{60}/d_{10}$) which is used in combination with D to characterize different initial sand grading.

Eq. (1) shows a complicated relation of B_r with five independent parameters, which would require a significant amount of effort to quantify the contribution of each parameter and their mutual dependence. In addition, the experiments performed in this study only involves calcareous sands in a very narrow size range (0.075-2 mm), and the derivation of a quantitative equation of B_r for sands with a wider particle size range can be even more difficult. Thus, to study the general trend of B_r, this section will only summarize the values of relative breakages obtained from tests performed in this study and relate them to the aforementioned parameters.

The relative breakages calculated from the PSD curves in Figure 7 for tests with different loading stress level (σ) and final shear strains (γ) are summarized in Figure 13. The results show that the degree of particle breakage increases with the final shear strain, and tends to remain constant at larger shear strains (> 4000%). The evolution of B_r with the shear strain can be described by linear and exponential functions for the low and high vertical loading stress levels, respectively. In addition, for a specific value of γ, the relative breakage of the specimen increases with the vertical loading stress. This phenomenon is as expected because the specimen can be densely consolidated under high vertical loads, and the increasing shear strain would cause continuous breakages of sands by particle asperities being sheared off. At large shear strains, the majority of calcareous sands were crushed into fine grains which would serve as a cushion layer to the relatively coarser sands nearby and resist further particle breakages (Einav (2007)). As it is difficult to crush the resultant fine particles under modest shear stresses, B_r would gradually converge to a constant value (see also the surface characteristics of shear bands in Figure 5 and Figure 6). This feature has also been observed in Coop et al. (2004), that very large strains are required for the tests to reach a stable relative particle breakage.

Figure 14 summarizes the relative breakage of calcareous sands with different initial grading for tests under vertical loading stresses of 50 kPa to 600 kPa. According to the figure, it can be observed that test RS-7 has a relatively large value of B_r under even very small loading stresses. In this case, the sand specimen has the same value of C_u as RS-5, but larger maximum grain size (D). The general trend shows that the particle relative breakage would increases with the maximum sand size, reflecting the fact that the coarse calcareous sands can be crushed readily due to their low shear strength. However, if D is fixed, the value of B_r will be inversely related to C_u (see the comparison between RS-7 and RS-8). In addition, tests RS-5 and RS-8 have almost the same B_r for low vertical stress (≤300 kPa), while at higher loading stress, B_r becomes larger for RS-5. For the case of RS-8, the well graded sand specimen with high coefficient of uniformity (C_u) can have a high packing efficiency, such that the coarse grains have very high coordination numbers with efficient force transferring. Consequently, the probability of particle breakage was significantly reduced. This is particularly evident for tests under high loading stress, because the specimen was densely consolidated. These results show that the initial well graded sand specimen can effectively resist breakage, because the proportion of coarse grains is relatively small, and the coordination number of coarse grains is relatively high. This result can match well the experimental observations by Altuhafi and Coop (2011) that uniformly graded and coarse sands would suffer catastrophic splitting under external loading, creating a large amount of fine grains. For all the tests, the relationship between B_r and vertical loading stress can be fitted well by exponential functions. In addition, for tests with different shear rates (e.g. RS-3, RS-9 and RS-10), the relative breakages are calculated as 0.281, 0.314 and 0.339, respectively. The result indicates that slow shearing of calcareous sands can lead to a high degree of particle breakage.

Conclusions

This paper presents experimental results of a series of ring shear tests with various initial conditions, e.g. loading stress level, sand grading and shear rate, to investigate the characteristics of particle breakage and the corresponding stress and strain evolutions. The main conclusions can be summarized as follows:

1) During the ring shear tests, the calcareous sand specimen dilates slightly at small shear strains, and then contracts continuously at large shear strains. The constant volumetric strain and stable particle grading could be reached at shear strains larger than 2000%. In addition, the residual shear stress increases with the vertical loading stress, and is independent of the material property and shear rate.

2) Particle breakage occurs readily during shearing and can continue to very large shear strains (e.g. > 2000%). It shows a gradual convergency towards a constant particle relative breakage. This value of constant relative breakage increases with the vertical loading stress and becomes larger for specimens with a uniform and coarse sand grading. The SEM images show clearly that the shear band consists of highly crushed fine grains, and the smoothness of the surface increases with the shear strain.

3) The analyses of particle size distribution for calcareous sands show that a large proportion of particles samller than 0.074 mm can still be crushed frequently under relatively small vertical loading stresses. The sizes of these fine particles can be measured by the laser diffraction particle size analyzer. Thus, the previously selected size limit of a silt in the definition of relative breakage can be further decreased to consider the breakage potential of finer particles.

Acknowledgements

This research was supported by the National Natural Science Foundation of China (grant 41372316 and 41572297), the opening fund of Key Laboratory of Geotechnical and Underground Engineering (Tongji University), Ministry of Education (grant KLE-TJGE-B1503), the Strategic Priority Research Program of the Chinese Academy of Sciences (grant XDA13010200), Youth Innovation Promotion Association of CAS (grant 2015272). All these supports are acknowledged.

References

Altuhafi, F. N., and Coop, M. R. (2011). "Changes to particle characteristics associated with the compression of sands." *Géotechnique*, 61(6), 459-471.

Bolton, M. D., Nakata, Y., and Cheng, Y. P. (2008). "Micro- and macro-mechanical behaviour of DEM crushable materials." *Géotechnique*, 58(6), 471-480.

Bowman, E. T., Take, W. A., Rait, K. L., and Hann, C. (2012). "Physical models of rock avalanche spreading behaviour with dynamic fragmentation." *Canadian Geotechnical Journal*, 49(4), 460-476.

Cho, G., Dodds, J., and Santamarina, J. (2006). "Particle Shape Effects on Packing Density, Stiffness, and Strength: Natural and Crushed Sands." *Journal of Geotechnical and Geoenvironmental Engineering*, 132(5), 591-602.

Coop, M. R., Sorensen, K. K., Freitas, T. B., and Georgoutsos, G. (2004). "Particle breakage during shearing of a carbonate sand." *Géotechnique*, 54(3), 157-163.

David, W. A., John, P. C., and Martin, D. L. (2011). "Sydney Soil Model. II: Experimental Validation." *International Journal of Geomechanics*, 11(3), 225-238.

Donohue, S., O'sullivan, C., and Long, M. (2009). "Particle breakage during cyclic triaxial loading of a carbonate sand." *Géotechnique*, 59(5), 477-482.

Einav, I. (2007). "Breakage mechanics—Part I: Theory." *Journal of the Mechanics and Physics of Solids*, 55(6), 1274-1297.

Fukuoka, H., Sassa, K., and Wang, G. (2007). "Shear Behavior and Shear Zone Structure of Granular Materials in Naturally Drained Ring Shear Tests." *Progress in Landslide Science*, K. Sassa, H. Fukuoka, F. Wang, and G. Wang, eds., Springer Berlin Heidelberg, Berlin, Heidelberg, 99-111.

Hardin, B. O. (1985). "Crushing of Soil Particles." *Journal of Geotechnical Engineering*, 111(10), 1177-1192.

Hyodo, M., Hyde, A. F. L., Aramaki, N., and Nakata, Y. (2002). "Undrained monotonic and cyclic shear behaviour of sand under low and high confining stresses." *Soils and Foundations*, 42(3), 63-76.

Lade, P., Yamamuro, J., and Bopp, P. (1996). "Significance of Particle Crushing in Granular Materials." *Journal of Geotechnical Engineering*, 122(4), 309-316.

Locat, P., Couture, R., Leroueil, S., Locat, J., and Jaboyedoff, M. (2006). "Fragmentation energy in rock avalanches." *Canadian Geotechnical Journal*, 43(8), 830-851.

Luzzani, L., and Coop, M. R. (2002). "On the relationship between particle breakage and the critical state of sands." *Soils and Foundations*, 42(2), 71-82.

McDowell, G. R., and Bolton, M. D. (1998). "On the micromechanics of crushable aggregates." *Géotechnique*, 48(5), 667-679.

McDowell, G. R. (2002). "On the yielding and plastic compression of sand." *Soils and Foundations*, 42(1), 139-145.

McDowell, G. R., Nakata, Y., and Hyodo, M. (2002). "On the plastic hardening of sand." *Géotechnique*, 52(5), 349-358.

Miao, G., and Airey, D. (2013). "Breakage and ultimate states for a carbonate sand." *Géotechnique*, 63(14), 1221-1229.

Muir Wood, D., and Maeda, K. (2007). "Changing grading of soil: effect on critical states." *Acta Geotech.*, 3(1), 3-14.

Qadimi, A., and Coop, M. R. (2007). "The undrained cyclic behaviour of a carbonate sand." *Géotechnique*, 57(9), 739-750.

Richard, P. J., Michael, E. P., Tuncer, B. E., Peter, J. B., and Nabil Ben, K. (2001). "DEM Simulation of Particle Damage in Granular Media — Structure Interfaces." *International Journal of Geomechanics*, 1(1), 21-39.

Sadrekarimi, A., and Olson, S. M. (2010). "Shear Band Formation Observed in Ring Shear Tests on Sandy Soils." *Journal of Geotechnical and Geoenvironmental Engineering*, 136(2), 366-375.

Sebastian, L.-G., Luis, E. V., and Luis, F. V. (2006). "Visualization of Crushing Evolution in Granular Materials under Compression Using DEM." *International Journal of Geomechanics*, 6(3), 195-200.

Shahnazari, H., and Rezvani, R. (2013). "Effective parameters for the particle breakage of calcareous sands: An experimental study." *Engineering Geology*, 159, 98-105.

Wang, X.-Z., Wang, X., Jin, Z.-C., Meng, Q.-S., Zhu, C.-Q., and Wang, R. (2017). "Shear characteristics of calcareous gravelly soil." *Bull Eng Geol Environ*, 76(2), 561-573.

Wang, X. Z., Jiao, Y. Y., Wang, R., Hu, M. J., Meng, Q. S., and Tan, F. Y. (2011). "Engineering characteristics of the calcareous sand in Nansha Islands, South China Sea." *Engineering Geology*, 120(1-4), 40-47.

Wu, Y., Yoshimoto, N., Hyodo, M., and Nakata, Y. (2014). "Evaluation of crushing stress at critical state of granulated coal ash in triaxial test." *Géotechnique Letters*, 4(4), 337-342.

Yu, F. W. (2017). "Particle Breakage and the Drained Shear Behavior of Sands." *International Journal of Geomechanics*, 17(8).

Zhang, S., Tong, C.-X., Li, X., and Sheng, D. (2015). "A new method for studying the evolution of particle breakage." *Géotechnique*, 65(11), 911-922.

Captions

Figure 1. The ring shear test apparatus. 's1': vertical loading load cell; 's2': vertical displacement dial gauge transducer; (a): shear box filled with calcareous sands; (b) shear box covered by porous stone disc and upper loading plate; (c), (d): shear box fixed on the testing rig.

Figure 2. Calcareous sands obtained at different stages of the ring shear tests

Figure 3. The shear stress and strain relationship of calcareous sands under various vertical loading stresses. The locations L-1, L-2, L-3 and L-4 correspond to the final shear strain of tests RS-1, RS-2, RS-3 and RS-4.

Figure 4. Evolution of volumetric strain with shearing strain for test RS-5 under various vertical loading stress.

Figure 5. Images of calcareous sand specimen after the RS tests. The figures (a) to (e) were obtained from tests RS-1 to RS-5 (see Table 1), respectively, showing the evolution of particle compositions with the shear strain. The shear band is delimited by enclosed red dashed curves.

Figure 6. SEM images of calcareous sand specimen after the RS tests (the vertical loading stress is 400 kPa). figure (a) is the image of a single coarse calcareous sand particle. Figure (b)-(f) are the results of tests RS-1, RS-2, RS-3, RS-4 and RS-5, respectively.

Figure 7. PSD of the calcareous sands in the shear band, (a), (b), (c) are results of tests under vertical loading stresses of 200 kPa, 300 kPa and 400 kPa, respectively. Figure (d) illustrates the definition of relative breakage, B_r, as the ratio of total particle breakage (area B) to the potential breakage (area A+B).

Figure 8. The relationship between shear stress and strain for calcareous sands with different initial sand grading under the vertical loading stress of 300 kPa.

Figure 9. Evolution of volumetric strain with the shearing strain for tests with different initial sand grading.

Figure 10. PSD of the calcareous sands in the shear band for tests with different initial sand grading.

Figure 11. The relationship between shear stress and strain for calcareous sands with various shear rates under the vertical loading stress of 300 kPa.

Figure 12. PSD of the calcareous sands in the shear band for tests with different shear rates.

Figure 13. The relationship between the relative breakage and shear strain for calcareous sands under various vertical loading stresses.

Figure 14. The relative breakage of calcareous sands with different initial sand grading.

Table 1. Details of the testing conditions.

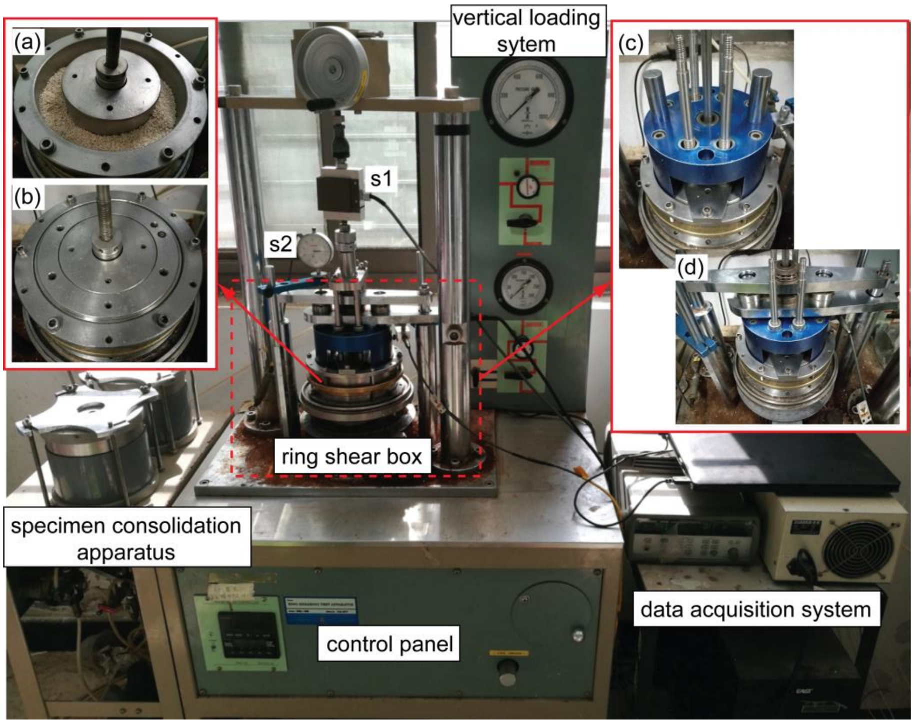

Figure 1. The ring shear test apparatus. ‘s1’: vertical loading load cell; ‘s2’: vertical displacement dial gauge transducer; (a): shear box filled with calcareous sands; (b) shear box covered by porous stone disc and upper loading plate; (c), (d): shear box fixed on the testing rig.

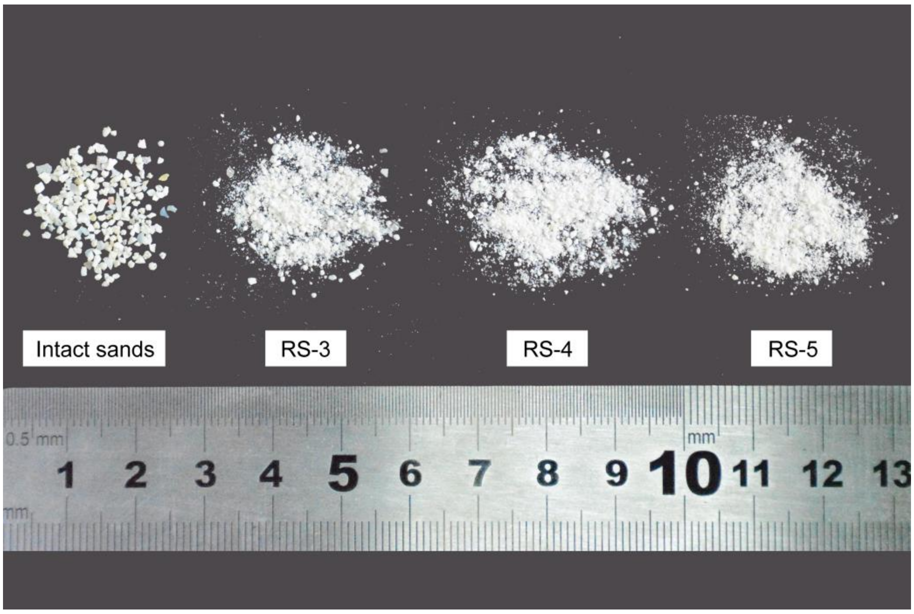

Figure 2. Calcareous sands obtained at different stages of the ring shear tests (the vertical loading stress is 300 kPa).

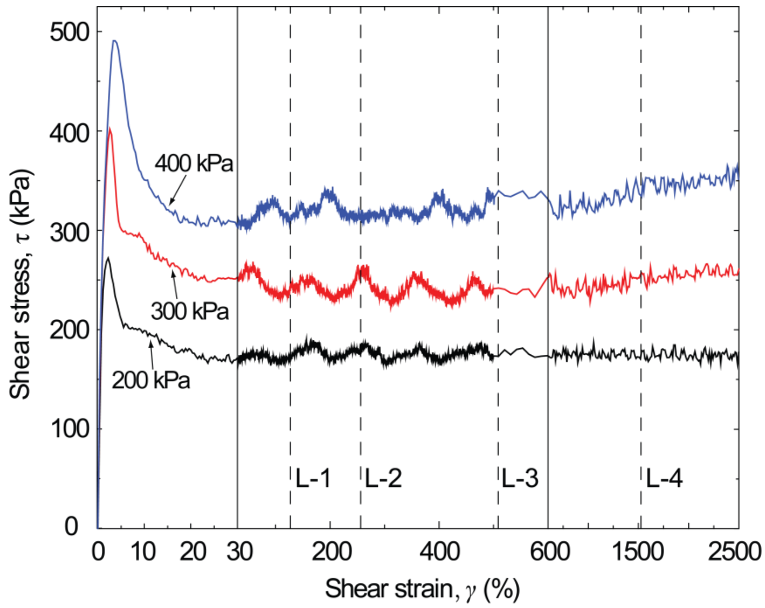

Figure 3. The shear stress and strain relationship of calcareous sands under various vertical loading stresses. The locations L-1, L-2, L-3 and L-4 correspond to the final shear strain of tests RS-1, RS-2, RS-3 and RS-4.

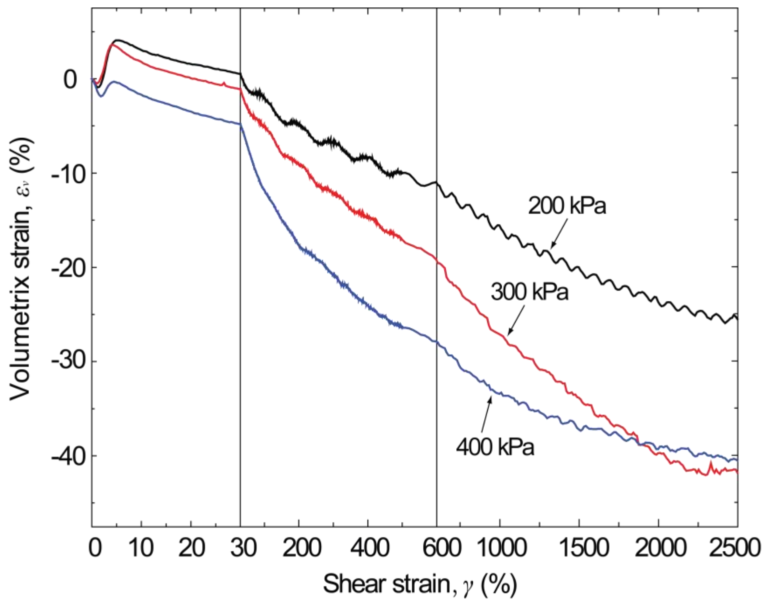

Figure 4. Evolution of volumetric strain with shearing strain for test RS-5 under various vertical loading stress.

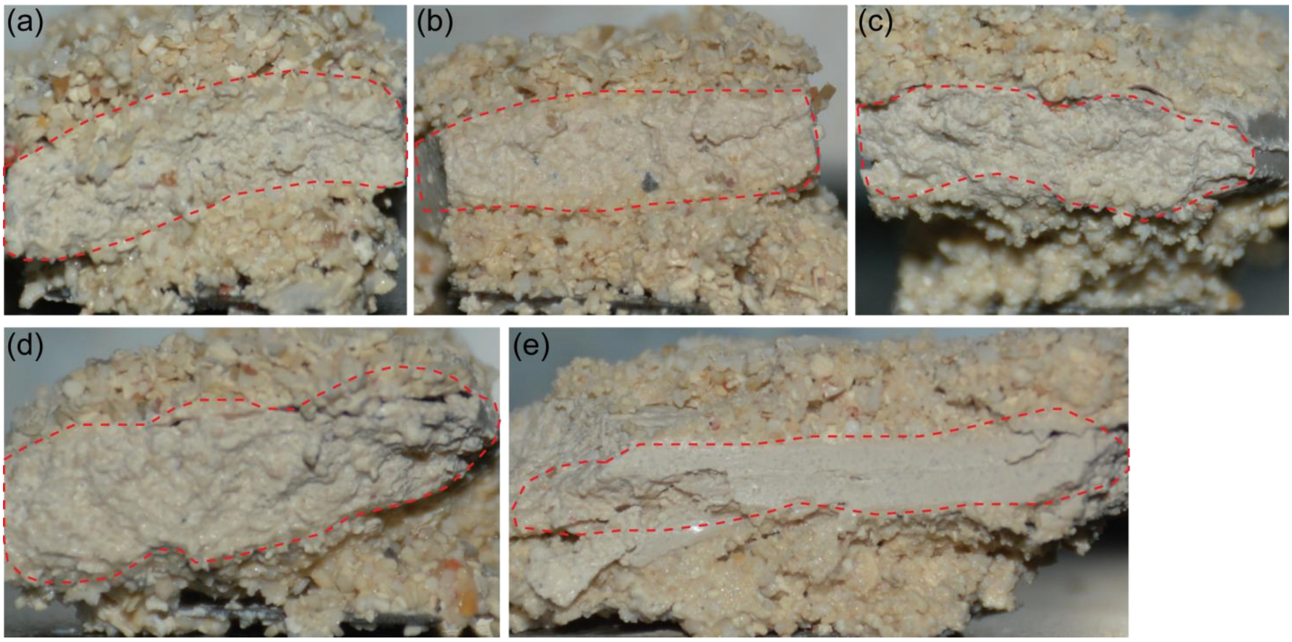

Figure 5. Images of calcareous sand specimen after the RS tests. The figures (a) to (e) were obtained from tests RS-1 to RS-5 (see Table 1), respectively, showing the evolution of particle compositions with the shear strain. The shear band is delimited by enclosed red dashed curves.The verticle loading stress is 400 kPa.

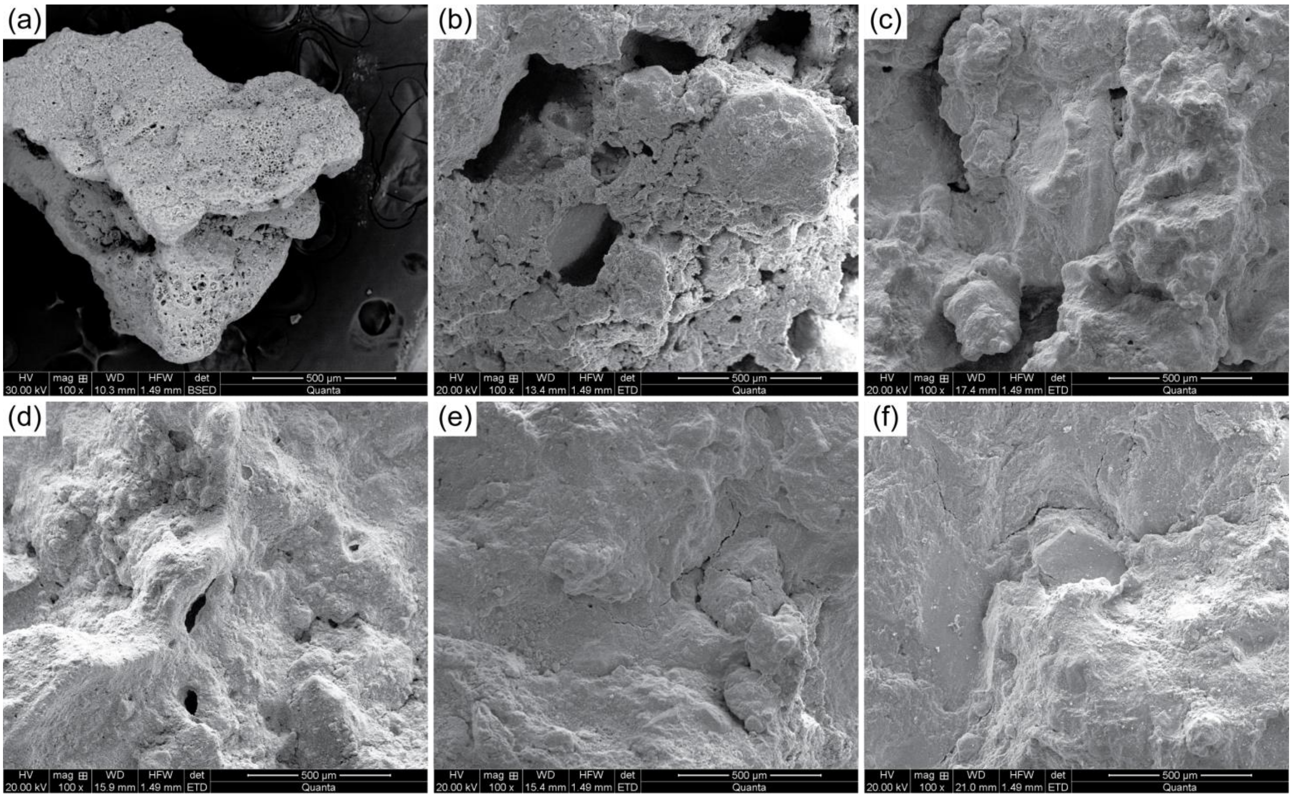

Figure 6. SEM images of calcareous sand specimen after RS tests (the vertical loading stress is 400 kPa). (a) is the image of a coarse calcareous sand particle. (b)-(f) are the results of tests RS-1, RS-2, RS-3, RS-4 and RS-5, respectively.

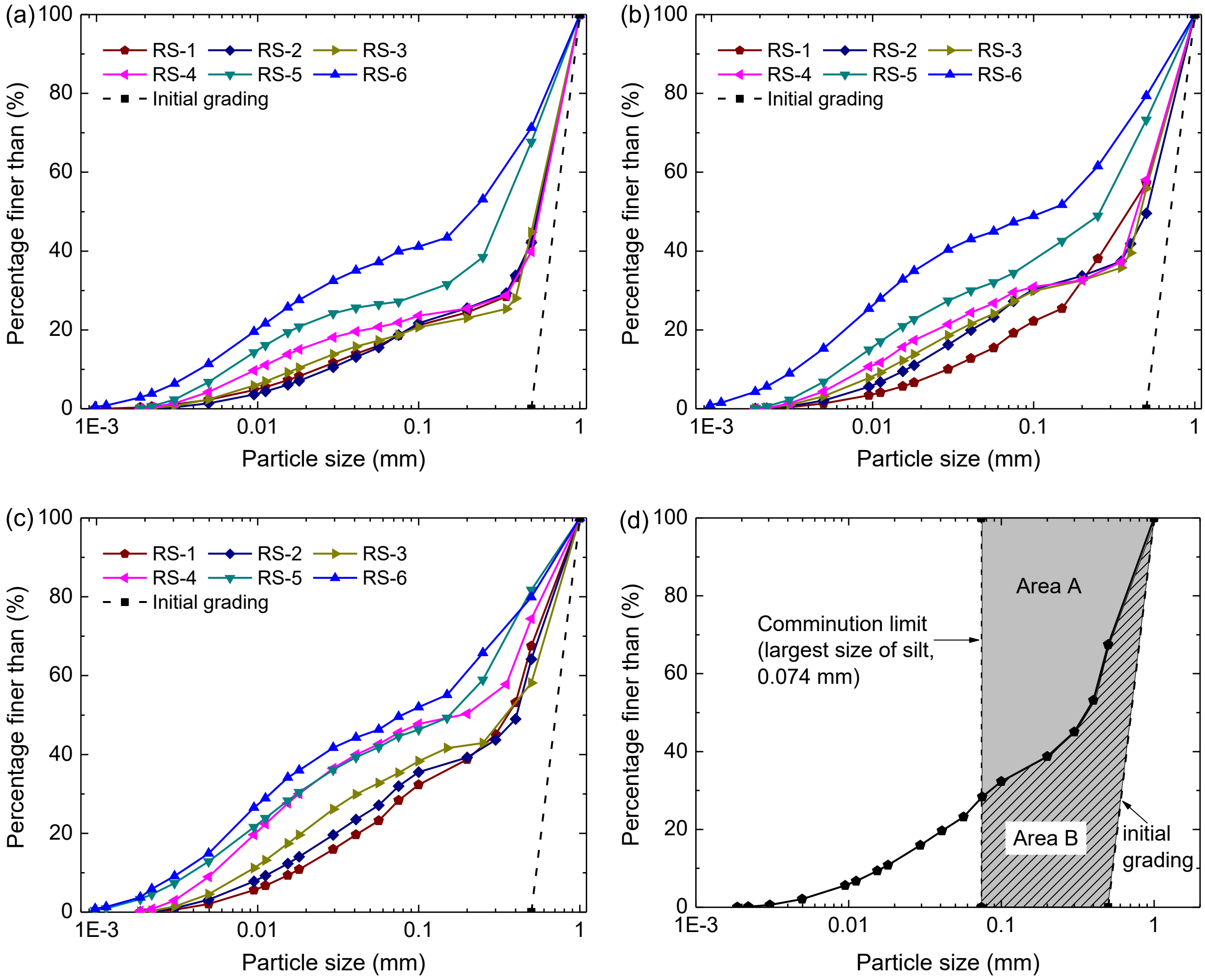

Figure 7. PSD of the calcareous sands in the shear band, (a), (b), (c) are results of tests under vertical loading stresses of 200 kPa, 300 kPa and 400 kPa, respectively. Figure (d) illustrates the definition of relative breakage, B_r, as the ratio of total particle breakage (area B) to the potential breakage (area A+B).

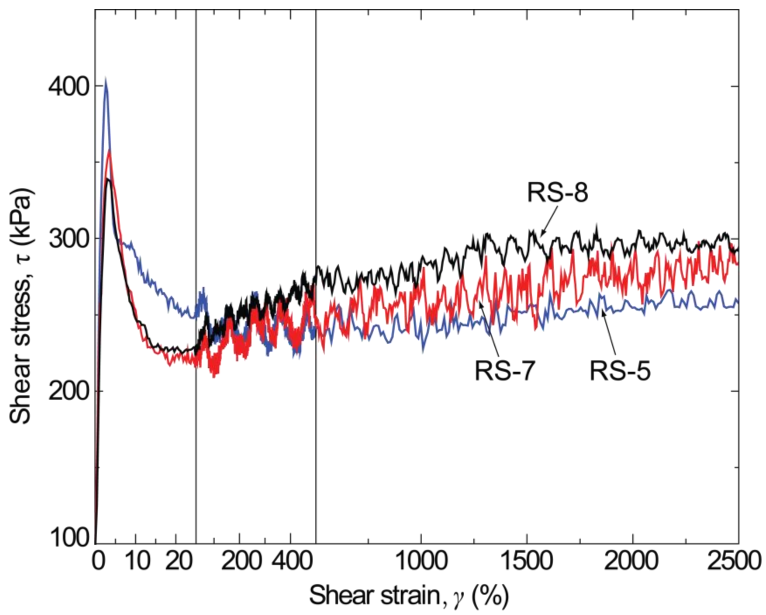

Figure 8. The relationship between shear stress and strain for calcareous sands with different initial sand grading under the vertical loading stress of 300 kPa.

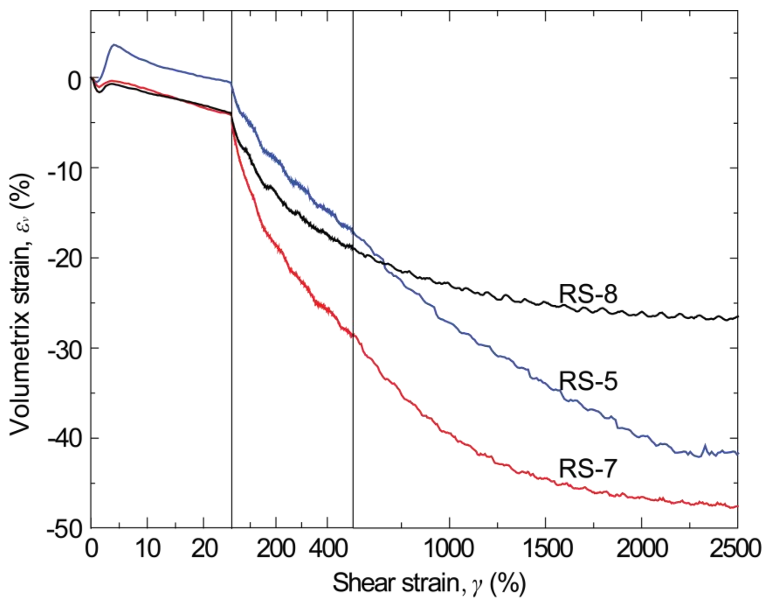

Figure 9. Evolution of volumetric strain with the shearing strain for tests with different initial sand grading.

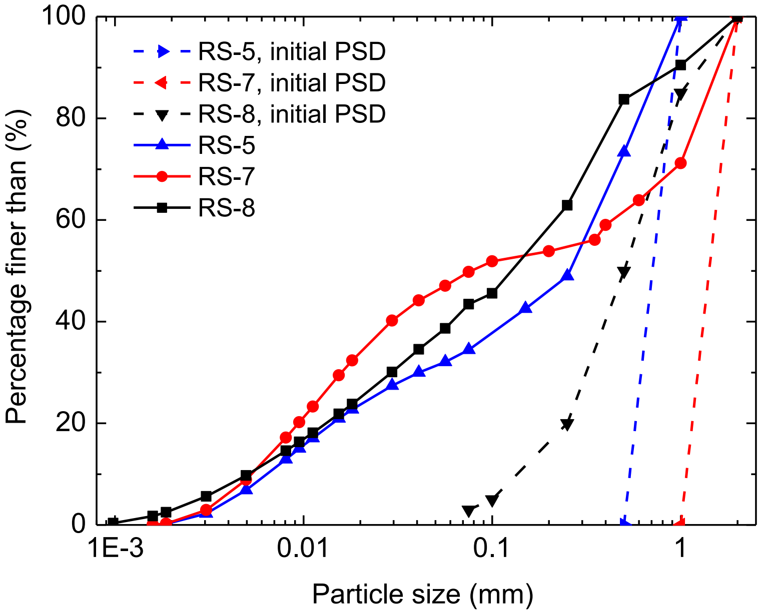

Figure 10. PSD of the calcareous sands in the shear band for tests with different initial sand grading.

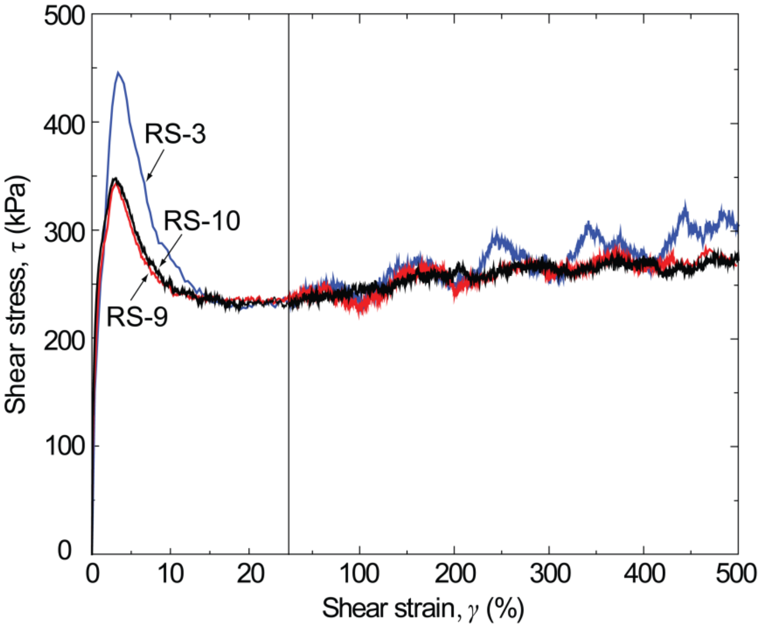

Figure 11. The relationship between shear stress and strain for calcareous sands with various shear rates under the vertical loading stress of 300 kPa.

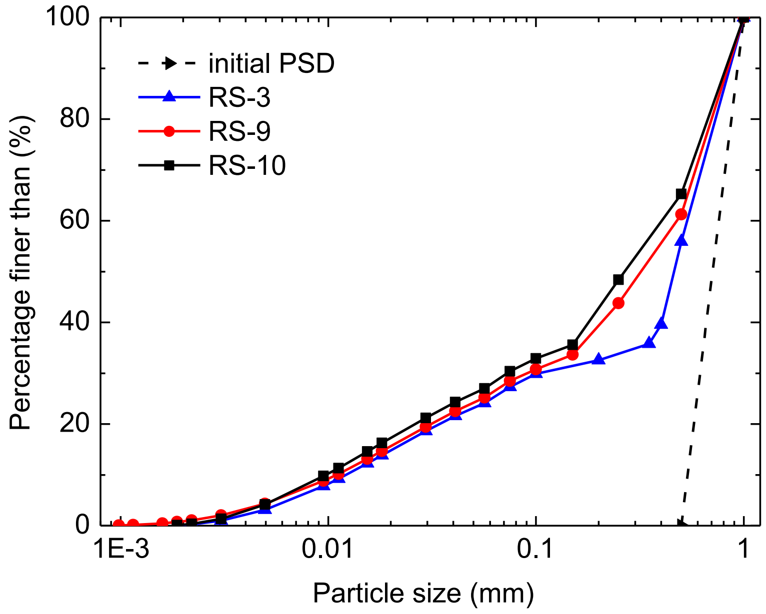

Figure 12. PSD of the calcareous sands in the shear band for tests with different shear rate.

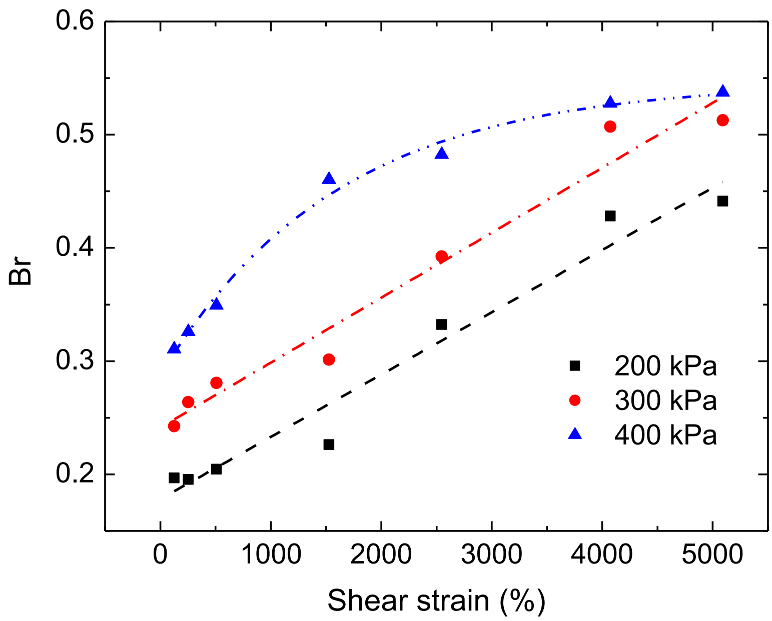

Figure 13. The relationship between the relative breakage and shear strain for calcareous sands under various vertical loading stresses.

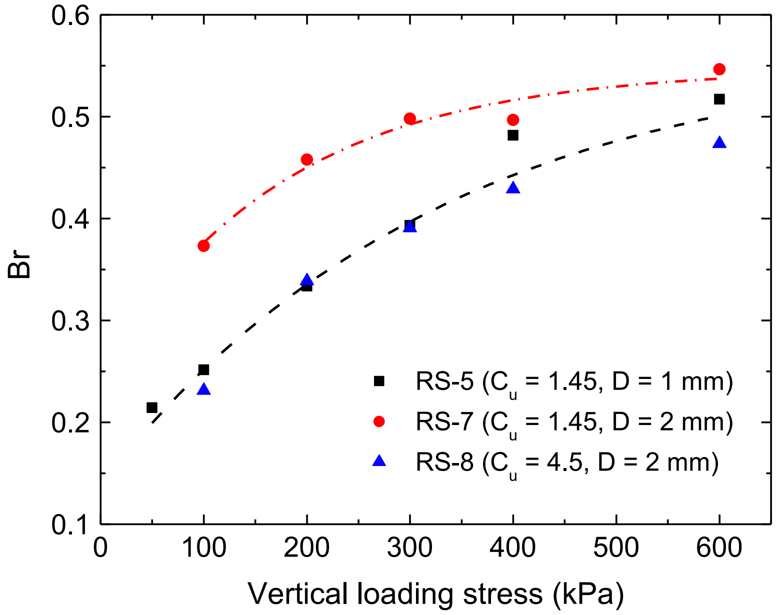

Figure 14. The relative breakage of calcareous sands with different initial sand grading.

Table 1. Details of the testing conditions.

Test	Initial grading: mm	Initial void ratio, e	Vertical load, σ_v: kPa	Shear rate: mm/min	Final shear distance: mm	Final shear strain: %
RS-1	0.5 - 1	1.71	200 - 400	43.6	500	127.3
RS-2	0.5 - 1	1.71	200 - 400	43.6	1000	254.6
RS-3	0.5 - 1	1.71	200 - 400	43.6	2000	509.3
RS-4	0.5 - 1	1.71	200 - 400	43.6	6000	1527.9
RS-5	0.5 - 1	1.71	200 - 400	43.6	10000	2546.5
RS-6	0.5 - 1	1.71	200 - 400	43.6	16000	4074.4
RS-7	1 - 2	1.66	300	43.6	10000	2546.5
RS-8	0.075 - 2	1.51	300	43.6	10000	2546.5
RS-9	0.5 - 1	1.71	300	11	2000	509.3
RS-10	0.5 - 1	1.71	300	3.3	2000	509.3